 FDMP, vol.4, no.4, pp.263-269, 2008

Towards a Numerical Benchmark for 3D Low Mach Number Mixed Flows in a Rectangular Channel Heated from Below

G. Accary[1], S. Meradji[2], D. Morvan[2] and D. Fougère[2]

Abstract: In the literature, only few references have dealt with mixed-convection flows in the low Mach number approximation. For this reason, in the present study we propose to extend the standard 3D benchmark for mixed convection in a rectangular channel heated from below (Medale and Nicolas, 2005) to the case of large temperature variations (for which the Boussinesq approximation is no longer valid). The Navier-Stokes equations, obtained under the assumption of a low Mach number flow, are solved using a finite volume method. The results, corresponding to the steady-state case of the benchmark, lead to the idea of launching a call for contribution (whose outlines still need to be defined) in order to set up a reference solution essential for the validation of future numerical codes.

Keyword: mixed convection, low Mach number, 3D benchmark, direct numerical simulation.

Nomenclature

g	Earth gravity, m.s^{-2}
H	Height of the channel, m
n	Mesh size
P_{th}	Thermodynamic pressure, Pa
R	Perfect gas constant, J.Kg^{-1}.K^{-1}
T	Temperature, K
U_m	Mean velocity at the inlet, m.s^{-1}
U,V,W	Non-dimensional velocity components
x,y,z	Coordinates, m
X,Y,Z	Non-dimensional coordinates

Greek Symbols

ε	Heating parameter, $(T_h - T_0)/T_0$
θ	Reduced temperature, $(T - T_0)/(T_h - T_0)$
κ	Thermal diffusivity, m^2.s^{-1}
μ	Dynamic viscosity, Pa.s
ρ	Density, kg.m^{-3}

Subscripts

0	Reference value
h	Hot boundary (the bottom one)

Non-dimensional Numbers

Nu	Nusselt number, $[-H(\partial T/\partial z)/(T_h - T_0)]$
Pr	Prandtl number, $[\mu_0/\kappa_0\rho_0]$
Re	Reynolds number, $[\rho_0 U_m H/\mu_0]$
Ra	Rayleigh number, $[PrgH^3\rho_0^2\varepsilon/\mu_0^2]$

1 Introduction

In the prospective of developing computation codes allowing the prediction of mixed-convection flows, one cannot rely on experimental data only (for checking the predicted result). Often it is necessary to model with a sufficient accuracy experimental conditions that are not always easy to control. This is why, in accordance with the approach used in Medale and Nicolas (2005) and in Le Quéré, Weisman, Paillère, Vierendeels, Dick, Becker, and Braack (2005), the validation of numerical codes requires setting up a well-defined benchmark, especially in the case of 3D mixed-convection.

Fluid flows in horizontal rectangular channels heated from below, also known as Poiseuille-Rayleigh-Bénard flows, are known to undergo a thermoconvective instability. This instability results in a mixed convection state whose complexity (as witnessed by the numerous control parameters and the related spatio-temporal structures), makes it very attractive for investigation (Nicolas, 1997; Nicolas, Luijkx, and Platten, 2000).

[1] USEK, Jounieh, Lebanon
[2] MSNM-GP, UMR 6181 CNRS, Marseille, France

The aforementioned complexity and variety of possible flow regimes make the Poiseuille-Rayleigh-Bénard configuration an interesting test case for checking the ability of numerical codes to predict mixed-convection flows.

Along these lines, the present study further refines and improves the benchmark previously defined in Medale and Nicolas (2005) for small temperature variations (Boussinesq assumption). Only the first part of the benchmark is treated here, that is to say the steady-state case. This case is extended to large temperature variations under the assumption of a low Mach number (Ma<0.3) for which, to our knowledge, no database for comparison exists yet.

2 Configuration

The proposed flow is a Poiseuille-Rayleigh-Bénard flow taking place in a horizontal channel heated from below of height H, width 10H, and length 50H, as shown in Fig. 1. The lateral vertical walls are insulated, while the horizontal ones are insulated over a length of 2H from the inlet section. Beyond this insulated zone, the horizontal top wall is maintained at a uniform temperature T_0 while the bottom one is maintained at a uniform temperature $T_h > T_0$. The space origin is placed at the distance of 2H from the inlet section, thus marking the transition between the insulated part of the horizontal walls and the isothermal part.

3 Modeling

We consider a Newtonian fluid whose flow is governed by the Navier-Stokes and energy equations obtained under the assumption of low Mach numbers (acoustic filtering, Paolucci (1982)) with the equation of state of a perfect gas. The acoustic filtering results in neglecting the viscous dissipation in the energy equation and in splitting the pressure in two independent parts: the dynamic pressure involved through its gradient in the momentum equations and the thermodynamic pressure (homogeneous in space) involved in the energy equation and in the equation of state. The transport equations, solved in their conservative form are not recalled here because the mathematical model is entirely described in Le Quéré, Weisman, Paillère, Vierendeels, Dick, Becker, and Braack (2005) or in Becker and Braack (2002). H, T_0, the mean value of the inlet velocity profile U_m, and H/U_m are chosen respectively as reference values for space, temperature, velocity, and time. This choice results in the non-dimensional numbers of Reynolds, Rayleigh, and Prandtl, given by:

$$Re = \frac{\rho_0 U_m H}{\mu_0}, \quad Ra = \frac{\mathrm{Pr}\, g H^3 \rho_0^2 \varepsilon}{\mu_0^2} \quad \mathrm{Pr} = \frac{\mu_0}{\kappa_0 \rho_0},$$

where $\varepsilon = (T_h - T_0)/T_0$ is the heating parameter, i.e. $T_h = (1+\varepsilon)T_0$, g=9.8 m.s^{-2} is the intensity of Earth gravity, κ_0 is the thermal diffusivity, μ_0 is the dynamic viscosity, $\rho_0 = P_{th0}/RT_0$ is the mean density, P_{th0} being the reference thermodynamic pressure. We also define a reduced temperature $\theta = (T - T_0)/(T_h - T_0)$.

As it will be shown later on, the density at the inlet section of the solution obtained in the low Mach number approximation is larger than ρ_0, unlike the Boussinesq assumption where density is supposed constant everywhere in the transport equations except for the buoyancy term. Consequently, the Reynolds number measured at the inlet will not be conserved if the value of U_m is kept constant.

Thus, two versions of the low Mach number approximation were considered in the present study. In the first version (case 1), we conserve the Reynolds number obtained from the reference parameters by adapting the value of U_m. In the second version (case 2), we maintain the inlet velocity profile but the Reynolds number will not be conserved. In both cases, the total mass of the fluid system ($500 \times \rho_0 H^3$) is conserved (confined flow) and the mean density in the domain is equal to ρ_0.

In accordance with the benchmark of Medale and Nicolas (2005), we consider air as working fluid (R=287 J.Kg^{-1}.K^{-1}, $\mu_0 = 1.68 \times 10^{-5}$ Pa.s, $Pr = 0.71$). The height of the channel H was taken equal to 1 cm, the reference temperature T_0 = 600 K, and the thermodynamic pressure of reference $P_{th0} = 1.013 \times 10^5$ Pa. At the inlet, we apply a uniform temperature T_0 and a Poiseuille-

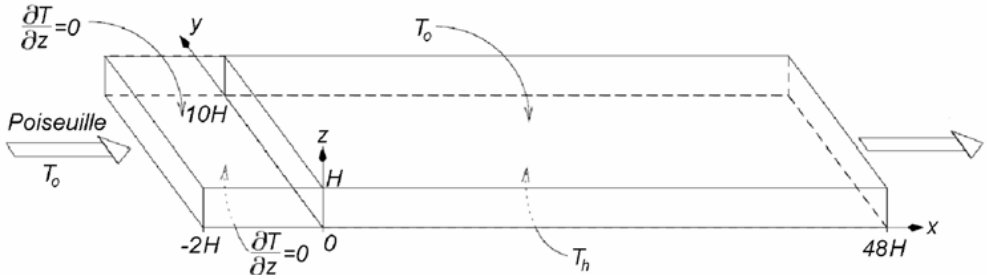

Figure 1: The configuration and the boundary conditions on the horizontal walls (the vertical lateral walls are insulated).

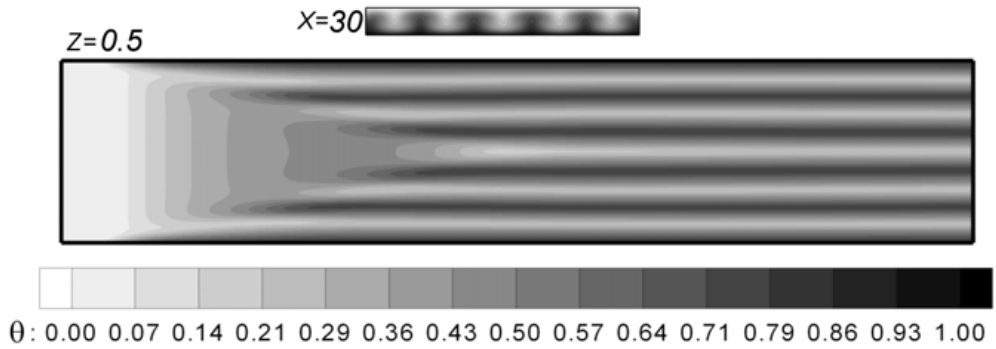

Figure 2: Slices of the reduced temperature field in the vertical plan ($X = 30$) and in the horizontal plan ($Z = 0.5$), obtained in the Boussinesq approximation.

type U-profile whose analytical expression can be found in Nicolas, Luijkx, and Platten (2000) and whose mean value U_m is determined through the Reynolds number. Finally, the parameter ε allows the choice of the Rayleigh number. The steady-state case of the benchmark of Medale and Nicolas (2005) (considered here) is characterized by $Re = 50$ and $Ra = 5000$; given the parameters mentioned above, this corresponds to U_m = 0.1427 m/s and ε=0.585 (large temperature variations).

4 Numerical aspects

The transport equations are solved by a fully-implicit finite volume method in a segregated formulation on a structured but non-uniform staggered mesh. The time discretization relies on a third order Euler scheme with variable time step. The space discretization is based on high order schemes with flux limiters: QUICK scheme (third order scheme) is used for convection terms while diffusion terms are approached by central difference approximation (second order).

The velocity pressure coupling is treated using SIMPLER algorithm and the linearization of the equations relies on the Picard procedure. The linear systems obtained from the discretised transport equations are solved using BiCGStab iterative method, while the linear system of the pressure equation (symmetric equation) is solved by the Conjugate Gradient (CG) method.

Since a steady state solution is sought, the transient term is dropped in all transport equations and the use of under-relaxation techniques allowed a faster convergence and better stability of the solution. A steady-state solution is supposed to be obtained when the residuals of all transport equations reach 10^{-10} in non-dimensional form.

The computations were carried out on an Itanium2 processor (1.5 GHz, 4 Mb of L3 cache memory). An OpenMP parallel version of the code is also available and is running on a SGI ALTIX cluster consisting in 20 Itanium2 processors and 40 GB of shared memory.

Initially, we apply uniform conditions: the Poiseuille velocity profile considered at the inlet boundary is applied everywhere in the computational domain, the fluid temperature is uniform and equal to T_0 and its density is equal to $\rho_0 = P_{th0}/RT_0$. All walls are solid boundaries, i.e. no slip conditions are applied to the dynamic field. For the temperature field, on the isothermal part of the horizontal walls ($X > 2$), uniform temperatures T_0 and $T_h = T_0(1+\varepsilon)$ are applied respectively on the top wall ($Z = 1$) and the bottom one ($Z = 0$). At the outlet ($X = 48$), a standard outflow condition is considered for all the primary variables, that is to say a Neumann condition ($\partial\Phi/\partial X = 0$, where $\Phi \equiv U, V, W$, and T).

In the staggered-mesh formulation, no pressure boundary condition is needed. For the U-component of the velocity, an additional treatment has been performed at the outlet together with the Neumann condition; at each iteration, the computed field of the U-component is corrected at the outlet boundary (multiplied by a constant) in order to retrieve the mass flow at the inlet. At convergence, both the mass conservation and the Neumann condition at the outlet are satisfied.

5 Validation

The numerical code described in section 4 was checked in the Boussinesq approximation by comparing the obtained results to those of the steady-state case of the benchmark (Medale and Nicolas (2005)). A quantitative agreement of the results was observed; this agreement required a non uniform mesh of ($n_x = 228$, $n_y = 182$ et $n_z = 80$), the mesh was refined near the solid walls and at the transition between the insulated zone and the isothermal one (at $X = 0$).

Convergence was reach after about 100 hours of CPU time. Since the purpose of the present study is not to answer, in details, to the call for contribution made in Medale and Nicolas (2005), we only present here a selection of the obtained results. Thus, we present in Fig. 2 the field of the reduced temperature θ in the vertical plan ($X = 30$) and the horizontal plan ($Z = 0.5$).

Figure 3 shows the profiles of the non-dimensional velocity components and of the reduced temperature along the axis ($Y = 5$, $Z = 0.5$). Figure 4 shows profiles of the Nusselt number, given by $Nu = -H(\partial T/\partial z)/(T_h - T_0)$, along the axis indicated on the figure itself. Figure 5 shows the mesh dependency of the solution; along the axis ($Y = 5$, $Z = 0.5$) and among all the primary variables, the U-component of the velocity presents the most important mesh dependency. For the two finest meshes ($n_z = 60$ and $n_z = 80$), the largest difference between the U-profiles shown in Fig. 5 is about 3%.

6 Comparison between formulations

As mentioned above, under the assumption of low Mach numbers, the selected test-case has two versions, the first one (case 1) consists in conserving the mass flow obtained from the reference values by adapting U_m, while in the second one (case 2) the inlet velocity profile is maintained. This leads, respectively, to the conservation of the Reynolds number (case 1) or to the conservation of the mean velocity at the inlet (case 2). As in the case of small temperature variations (Boussinesq), steady-state solutions were obtained for both versions of the low Mach number approximation and a converged solution (with a stopping criterion of 10^{-10}) was reach after about 250 hours of CPU time.

Figure 6 shows the evolution of the component U of the velocity along the axis ($Y = 5$, $Z = 0.5$) in the low Mach number approximation, compared to the solution obtained for small temperature variations (Boussinesq).

Because of the fluid system confinement, the total mass of the system is conserved and the mean density in the computational domain is equal to its reference value ρ_0. Now because of the heating applied to the bottom wall, the mean temperature in the channel increases. With the constraint of total mass conservation, the thermodynamic pressure increases of about 23% (here) for both versions of the low Mach number approximation (more precisely, P_{th}/P_{th0} = 1.2368 for case 1 and 1.2319 for case 2). At the inlet section of the domain (isothermal boundary), this results in an increase of the density according to the perfect gas

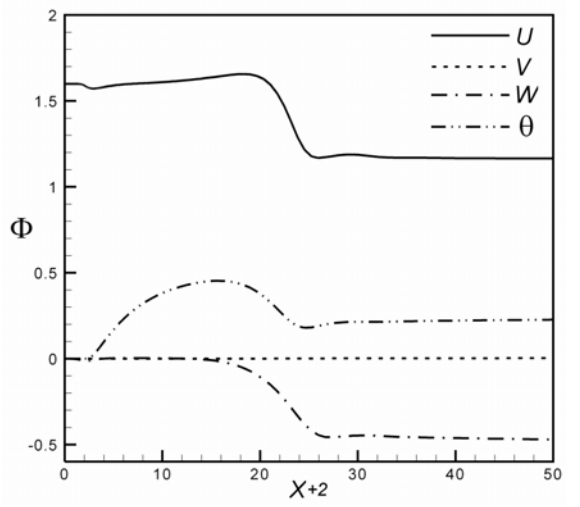

Figure 3: Profiles of the primary variables U, V, W, and θ along the axis ($Y = 5$, $Z = 0.5$) obtained in the Boussinesq approximation.

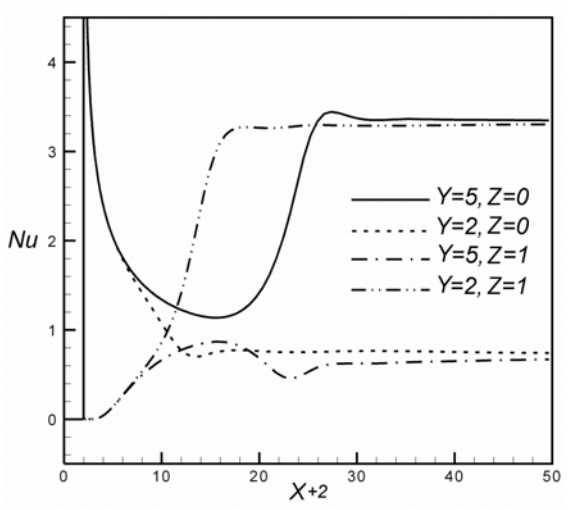

Figure 4: Evolution of the Nusselt number, obtained in the Boussinesq approximation, along different axis in the X direction.

equation of state ($\rho = P_{th}/RT$). Consequently, in case 1, we notice in Fig. 5 (a) that the mean velocity at the inlet is smaller than that of the Boussinesq approximation. In case 2, we notice a global increase in the inertial effects, which is directly related to the increase of the Reynolds number.

Important differences were observed between the

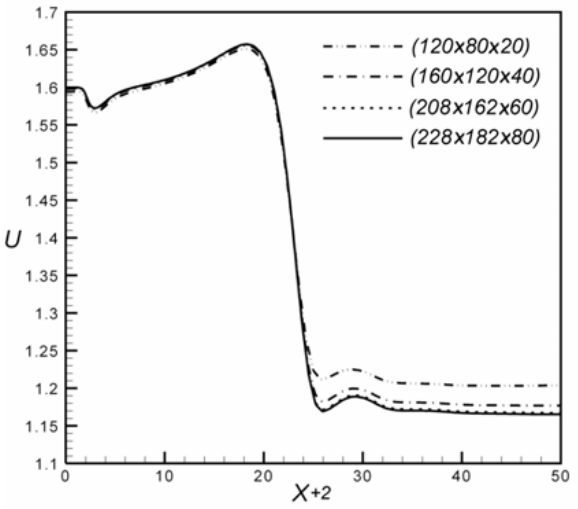

Figure 5: Profiles of the U-component of the velocity along the axis ($Y = 5$, $Z = 0.5$), obtained in the Boussinesq approximation using different meshes.

Boussinesq assumption and the low Mach number approximation on the dynamic field; however, at this stage of the investigations, it seems that the thermal field is less influenced by the choice of the formulation, as shown by Fig. 6 (b) presenting the profile of the reduced temperature. This can also be seen in Figs. 7 where the distributions of the Nusselt number on the bottom wall ($Z = 0$) and the top one ($Z = 1$) are presented along the median axis (Y=5). We notice also that in the low Mach number approximation, the choice of case 1 or case 2 does not have much impact on the temperature field at the outlet of the domain where the flow is practically established. Of course, further investigations still need to be carried out in order to confirm the well-founded choices made in this section (especially as far as the outflow condition is concerned). Finally, even though the convergence and the mesh dependence of the solution were carefully checked, the comparison with other solutions predicted by different methods, following the approach used in Medale and Nicolas (2005), is necessary.

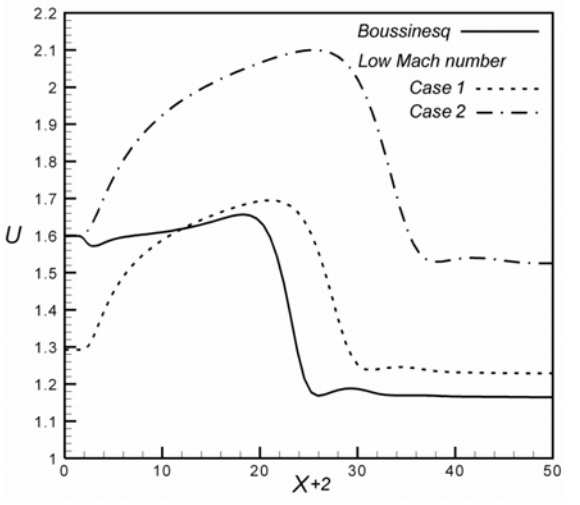

(a)

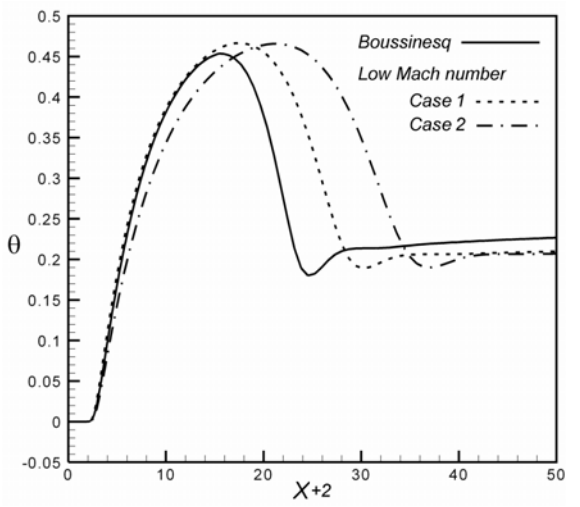

(b)

Figure 6: Profiles of the X-component of the velocity (a) and of the reduced temperature (b) along the axis ($Y = 5, Z = 0.5$) under the Boussinesq assumption and for the two considered cases of the low Mach number approximation (case 1: Re is conserved, case 2: U_m is conserved).

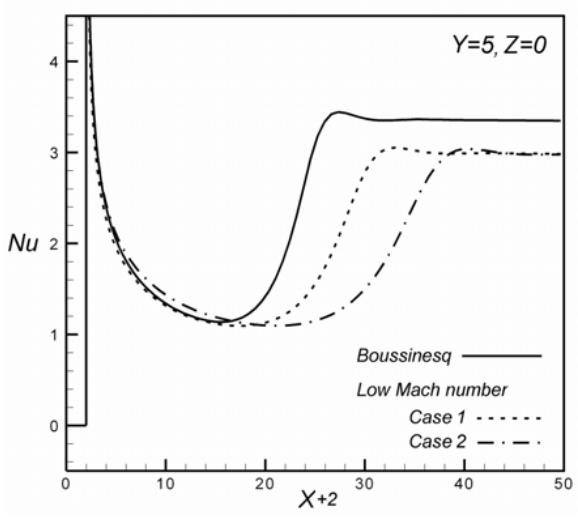

(a)

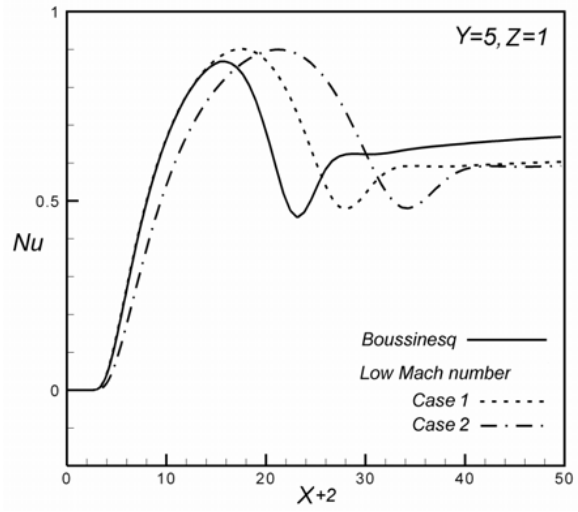

(b)

Figure 7: Distribution of the Nusselt number on the bottom wall (a) and on the top wall (b) along the median axis ($Y = 5$) in the Boussinesq assumption and for the two considered cases of the low Mach number approximation (case 1: Re is conserved, case 2: U_m is conserved).

7 Conclusion

Steady-state reference solutions were obtained for the Poiseuille-Rayleigh-Bénard problem in the case of large temperature variations ($\varepsilon = 0.585$) for $Re = 50$, $Ra = 5000$, and $Pr = 0.7$.

The authors are conscious of being at an embryonic stage of the procedure turning the present configuration into a benchmark. However, the important differences observed with respect to the solution obtained in the framework of the Boussinesq approximation justifies launching a call for contribution. This will be used to define the out-

lines of the work to be done and, subsequently, to obtain a reference solution for the validation of numerical codes developed under the assumption of a low Mach number, which must be regarded as an essential step before tackling complex physical configurations.

Acknowledgement: The authors thank the European community for the financial support in the context of Fireparadox project aiming to model the behavior of wild forest fire.

References

Becker, R.; Braack, M. (2002): Solution of a stationary benchmark problem for natural convection with large temperature difference. *Int. J. Thermal Sciences*, vol. 41, pp. 428-439.

Le Quéré, P.; Weisman, C.; Paillère, H.; Vierendeels, J.; Dick, E.; Becker, R.; Braack, M.; Locke, J. (2005): Modelling of natural convection flows with large temperature differences: A Benchmark problem for Low Mach number solvers. Part 1: Reference Solutions. *Mathematical Modelling and Numerical Analysis*, vol. 39, no. 3, pp. 609-707.

Medale, M.; Nicolas, X. (2005): Towards benchmark solutions for three-dimensional mixed convection flows in rectangular channels heated from below. *Conference of the French Thermal Society*. (http://www.sft.asso.fr/groupes/simul.html).

Nicolas, X. (1997): Simulation numérique et stabilité des écoulements de convection mixte en conduite rectangulaire chauffée par le bas. *Thesis at Université Paul Sabatier*.

Nicolas, X.; Luijkx, J. M.; Platten, J. K. (2000): Linear Stability of mixed convection flows in horizontal rectangular channels of finite transversal extension heated from below. *International Journal of Heat and Mass Transfer*, vol. 43, pp. 589-610.

Paolucci, S. (1982): On the filtering of sound from the Navier-Stokes equations. *Technical report, Sandia National Laboratories USA*, SAND82-8257.

Versteeg H.; Malalasekera W. (1995): An introduction to Computational Fluid Dynamics: The Finite Volume Method, *Longman*, Chap.9, pp. 198.